Research Report
KTC-88-5

Fatigue Analysis of the I-75 Bridge Over the Kentucky River at Clays Ferry

by

Theodore Hopwood, II
Chief Research Engineer

and

Vishwas G. Oka
Transportation Research Engineer I

Kentucky Transportation Center
College of Engineering
University of Kentucky
Lexington, Kentucky

in cooperation with
Law Engineering

October 1988

Technical Report Documentation Page

1. Report No.	2. Government Accession No.	3. Recipient's Catalog No.
KTC-88-5		

4. Title and Subtitle
Fatigue Analysis of The I 75 Bridge over The Kentucky River at Clays Ferry

5. Report Date
October 1988

6. Performing Organization Code

7. Author(s)
Hopwood, T. and Oka, V. G.

8. Performing Organization Report No.
KTC-88-5

9. Performing Organization Name and Address
Kentucky Transportation Center
College of Engineering
University of Kentucky
Lexington, KY 40506-0043

10. Work Unit No. (TRAIS)

11. Contract or Grant No.

12. Sponsoring Agency Name and Address
Law Engineering
11125 Decimal Drive
Louisville, KY 40299

13. Type of Report and Period Covered
FINAL June-October 1988

14. Sponsoring Agency Code

15. Supplementary Notes
Law Engineering Contract Officer: Steven D. Tucker

16. Abstract

Fatigue analysis was performed on AASHTO category E welded connections on the southbound I 75 bridge over the Kentucky River at Clays Ferry, Kentucky. That analysis was based on the stress-range histogram data provided by Law Engineering of Louisville, Kentucky. That data were obtained from strain gages installed at 6 test locations on the downstream truss.

The fatigue analyses consisted of safe-life and fatigue-crack growth analyses. Safe-life predictions were based on AASHTO fatigue design (SN) curves. To use those curves, equivalent constant-amplitude stresses were derived from the stress histograms. Those stresses and loading frequencies were modified to reflect anticipated increases in traffic volume and loading over the life of the structure by appropriate multiplicative adjustment factors. Four different methods of load prediction were used with combinations of the stress summing methods, total traffic, and truck traffic. In the majority of cases, the safe-life estimates exceeded 50 years. One overly conservative load-prediction method provided safe-life estimates as low as 15 years.

Continued on next page.

17. Key Words	18. Distribution Statement
Bridge Cracking Fatigue Steel Strain Gage	Unlimited with approval of Law Engineering

19. Security Classif. (of this report)	20. Security Classif. (of this page)	21. No. of Pages	22. Price
Unclassified	Unclassified	37	

Fatigue-crack growth analyses were performed at each test location using iterative crack-growth calculations by computer. The software program employed for that purpose required assumptions regarding initial and final size of the crack, crack geometry, and material properties. Analyses of hypothetical cracks at each test location was performed assuming a 1-inch initial size and a 6-inch final size. The fatigue-crack growth analyses predicted very slow growth of the cracks over that crack-length interval. For the present loading rates, those crack-length interval growth rates exceeded 350 years at all test locations.

The fatigue analyses indicated that the six test locations (gusset connections) were in a reasonably reliable condition from a fatigue standpoint to allow their continued use in the bridge over the next 50 years. Supplemental inspections, analyses and, possibly, gusset retrofits are warranted if the truss is to be retained in the new bridge. Existing cracks in the gusset connections should be repaired to preclude further crack growth.

INTRODUCTION

In June 1988, Law Engineering Company of Louisville, Kentucky contracted with the Kentucky Transportation Center (KTC) to provide technical assistance for installation of strain gages on the southbound I 75 bridge over the Kentucky River at Clays Ferry, Kentucky and analyses of the resulting strain-gage data. Law Engineering was responsible for installing strain gages and acquiring data at the test sites. Those tasks were part of a comprehensive inspection of the structure that was coordinated by Wilbur Smith and Associates (WSA) of Lexington, Kentucky. Prior to the contract with Law Engineering, KTC personnel assisted WSA in defining the scope of testing and also in selecting the necessary strain-gage equipment.

Due to the advanced age of southbound bridge (22 years), the presence of fatigue-prone weld details and the need to ensure a safe structure for future use, the Kentucky Department of Highways (KYDOH) requested a fatigue analysis of specific details on the bridge. The work entailed fatigue analyses of gusset plate to girder fillet welds in tension areas of the upper and lower chords and the bracing members of the three-span continuous truss. Those connections are AASHTO category E fatigue details. The fatigue susceptibility of that category of weld detail is high. The fatigue analysis was to be based on live-load stresses measured by strain gages installed on the downstream truss of the structure. KYDOH considered that only downstream truss needed gaging and analyses, as it would probably experience the highest live loads primarily due to truck traffic. Six test locations were specified by KYDOH based upon stress analyses that identified structural members having high live-load stresses. KYDOH assumed that similar structural connections on the bridge would perform no worse than those specified for gaging and analyses.

The strain-gage tests were intended only for analyses of fatigue-susceptible weld details. Those tests were not intended for detailed stress analyses. By convention of structural analysis, trusses are supposed to have only uniaxial forces in their members. To avoid any effects of secondary bending moments at the connections and to measure only uniaxial stresses, the strain gages were located on the structural members away from the connections. For the fatigue analyses, only the stress-range data were considered pertinent. Therefore, exact peak/valley stress values were not required. The fatigue analyses required data collection over an extended time period to

ensure that representative live-load stresses and frequency of load applications (stress cycles per time) were measured. A one-week test period was deemed sufficient considering the constraints of funding and time.

The tests required unattended data acquisition for extended time periods. As the measurement of a large number of stress cycles was anticipated, a stress-range measuring/recording system was necessary. The system that best met the test requirements was the "SoMat 2000 Portable Data Acquisition, Display, and Analysis System" (hereafter referred to as "SoMat"), manufactured by the SOMAT Corporation of Champaign, Illinois. It was a battery-powered, solid-state, one-channel system. It contained electric circuitry (analog and digital) to: power and measure analog strain-gage signals, conduct peak/valley strain-gage measurements, count and store resulting stress ranges in pre-selected stress-range histograms, and provide the time interval over which the measurements were taken. Two SoMat units were acquired along with a laptop computer to provide test settings and recover data after a field test was completed.

LABORATORY TESTING

KTC investigators assisted Law Engineering personnel in preparing the SoMats for field testing. Included in that work was laboratory calibration and testing of the SoMats.

Welded strain gages (with the same gage factor as those used on the I 75 bridge) were attached to a 1-inch wide by 1/4-inch thick steel bar. A half-bridge configuration was used with a dummy (temperature-compensating) gage mounted transversely to and an active gage mounted along the longitudinal axis of the bar. The bar was placed on an Instron screw-type universal test machine at the University of Kentucky Department of Material Science and Engineering Laboratory (Figure 1). The gages were connected to a SoMat and the unit was calibrated by loading the bar to known stresses between 0-30 ksi. Both SoMat units were calibrated in that manner. The histogram stress ranges in each SoMat memory were set at 1-ksi increments from 0 to 30 ksi.

The SoMats were tested for complete function by stress cycling the steel bar for three cycles at 3, 6, and 15 ksi. The data were recalled from the stress-range histogram memory of each SoMat and the correct number and magnitudes of the stress cycles were verified.

The SoMats were then taken to the bridge by Law Engineering personnel and employed on several test sites. Those initial tests revealed many stress cycles less than 5 ksi and a few stress cycles in excess of 10 ksi. Some of those higher stress range values exceeded 30 ksi. Those stress ranges were improbable. Therefore, KTC personnel contacted SOMAT Corporation personnel who then sent their representative to Lexington to investigate the problem. Prior to his arrival, KTC personnel discerned that the SoMats were susceptible to electrical interference due to either electromagnetic or radio-frequency fields. That interference would induce electrical signals into the strain-gage wires and would produce false stress-range data in SoMats. Those false stress-range indications could not generally be separated from valid data. Only the obviously incorrect values could be detected.

The SOMAT representative was appraised of the electrical noise problem. He took the two units to his laboratory for revision. They were subsequently equipped with 100-hertz, low-pass filters. The SOMAT representative requested that shunt calibration be used for stress calibration of the units. For that type of calibration, a known resistance internal to a SoMat is applied across the gages and the instrument span is set based upon the formula:

$$u_e = \frac{1}{K} \frac{Rg}{(Rcal+Rg)} \times 10^6 \qquad (1)$$

where

u_e = strain (in units of microstrain)
K = gage factor
Rcal = shunt resistance (ohms)
Rg = gage arm resistance (ohms).

Subsequently, a 100 k-ohm resistor could be connected externally across the gages in the field to produce a known strain reading given by the equation:

$$u_e = \frac{1}{K} \frac{\Delta R}{Rg} \times 10^6 \qquad (2)$$

where

ΔR = resistance applied across the gage arm and lead wires (ohms).

That test combined with the shunt calibration allowed verification that bridge-mounted gages were properly wired to a SoMat and that they provided correct strain values.

The field tests were conducted from July to August 1988 at the six test locations on the bridge. Tests were repeated at two locations where the SoMats suffered premature battery failures during earlier tests. Data were acquired at each location for a minimum of one week. Thereafter, the SoMats were returned to the University of Kentucky Department of Material Science and Engineering Laboratory and the shunt-calibration derived stresses were compared with the stresses determined by loading the gaged bar (Figure 2). Over the stress range of interest in this study, the shunt calibration provided stress values about 10 percent higher than the actual stresses as determined from the load test on the gaged bar. That meant the field-test values obtained from the shunt-calibrated gages were conservative and may have compensated for any error in strain-gage alignment on the bridge members.

FATIGUE ANALYSES

The fatigue analyses consist of two parts: 1) safe-life analyses for determining fatigue susceptibility and 2) fatigue-crack growth analyses of hypothetical flaws using fracture mechanics calculations to determine the inspection requirements.

Safe-life analyses provide an estimate of the remaining life of a structure. Those are based upon comparison of the cumulative aging or a damage that a structural detail of a bridge will incur due to service loads over its anticipated service life compared to the laboratory-derived performance of similar structural details in an equivalent loading environment.

Fatigue-crack growth analyses performed in this study are based upon the growth of a hypothetical crack of an assumed initial size to some predetermined critical crack size believed sufficient to cause failure (or a severe structural damage). Fatigue-crack growth equations are used for those analyses. Those equations incorporate structural member dimensions, material yield strength, initial size of a hypothetical crack, its disposition, and stress-range values provided by strain-gage tests. Fatigue-crack growth analyses provide an estimate of the necessary inspection sensitivity and frequency.

As noted, the strain-gage derived live-load stresses are believed to be conservative. Also, those strain-gage tests were conducted at locations on the truss where KYDOH analyses indicated maximum live-load stresses. Therefore, the following fatigue analyses are believed to provide "worst-case" predictions of structural integrity or crack growth.

The complete stress-range data were furnished by Law Engineering on August 29, 1988. They are listed in Table 1. 1-ksi increment stress ranges were used for all tests except for test locations 2 (L4L6-new test) and 5 (L14L16) where 1.2-ksi increments were necessitated by the SoMat calibration software.

A review of data indicates that a majority of stress cycles occur in the 0 to 1-ksi stress range. A few cycles were encountered at stress ranges above 5 ksi. However, those occurred infrequently during the one-week monitoring periods (less than 10 cycles at all test locations). The number of cycles in the 0 to 1-ksi stress range varied by a factor of about 10 among the test sites. In part, that is due to the way each member assumes live-load stresses and also, in part, due to the traffic patterns that vary across the bridge. That variance is caused by the length and inclination of the bridge. A few high stress-range cycles (above 30 ksi) were recorded at test location 1 (U3L4). Those were neglected since they were obviously due to electrical noise and are not presented in Table 1. The noise filters provided in the revised SoMats were not completely effective in eliminating noise problems as noted by the few high stress-range values recorded at that test location. However, the filtering proved effective at the other test locations.

SAFE-LIFE ANALYSES

Safe-Life analyses are typically applied to nonredundant structures. Implicit assumptions for safe-life analysis are: 1) the structure contains no fabrication defects when placed in service, 2) the performance of the major structural details are known in typical service environments, and 3) the service loads are within the limits specified by codes and accommodated for by design. The first assumption is verified in part by nondestructive testing (NDT) of high-risk welded connections in the fabrication shops to preclude fabrication defects. The second assumption is based in part on practical experience and also on full-scale laboratory fatigue testing of typical welded structural details (from which the AASHTO fatigue design curves are derived).

The third assumption is based on initial review of design calculations and can be confirmed by field strain gaging.

The presence of any factor negating any of the initial safe-life assumptions (such as undetected crack induced during fabrication or continuous overloading of a structure) would invalidate safe-life analyses. Thereafter, structural integrity would need to be assessed based on a combination of analyses using fracture mechanics and NDT.

To determine safe lives of the bridge members, the stress-range data acquired from the different test locations had to be resolved in to equivalent single-valued constant-amplitude stress ranges. The root-mean square (RMS) and the root-mean cube (RMC or Miner) summing methods were used.

The RMS method is given by equation:

$$Sre_{rms} = (\Sigma \, Pi \, Sri^2)^{1/2} \qquad (3)$$

where

Sre_{rms} = root-mean square or RMS equivalent stress
Pi = proportion of stress cycles for Sri, and
Sri = pre-selected stress range.

The RMC method is given by the equation:

$$Sre_{rmc} = (\Sigma \, Pi \, Sri^3)^{1/3} \qquad (4)$$

where

Sre_{rmc} = root-mean cube or RMC equivalent stress.

Those summing equations are discussed in a recent KTC report (1). The RMS equation correlates better with test data. The RMC equivalent stresses are typically about 10 percent higher than RMS equivalent stresses yielding more conservative fatigue analyses.

The resolved single-valued stresses are listed in Table 2. Those stresses are compared to results of constant-amplitude fatigue tests employed to derive AASHTO fatigue design curves (listed in tabular form in the Appendix). The AASHTO provision for nonredundant members were used whereby the test curves were shifted one range of loading cycles for the allowable stress-range values in each category. For the category E weld details, the allowable stress amplitude (endurance limit) for service lives over 2,000,000

cycles is 2.5 ksi.

The safe-life analyses had to consider past, present, and future service loads. A memorandum from the KYDOH Division of Planning (2) indicated that both the traffic volume in terms of average daily traffic (ADT) and the weight of traffic in terms of equivalent axle loads (EALs) was expected to increase through the year 2007. The increase in loading was attributed to future increases in both traffic volume and the percentage of trucks.

It was necessary to forecast future traffic using the bridge for the next 50 years, to anticipate its safe-life if incorporated in a widened six-lane structure. Linear regression was used to derive ADT and EAL growth equations based upon the Division of Planning traffic data. Those growth equations were used to predict ADT and EAL values to the year 2038. It was assumed that EALs are directly proportional to the stress ranges and ADTs to the number of load or stress cycles. ADT and EAL adjustment factors were calculated by dividing average ADT and EAL values by projected ADT and EAL values for the year 1988. The same exercise was repeated for the average daily truck traffic (ADTT) and truck EALs to obtain corresponding ADTT and EAL adjustment factors. Those are listed in Table 3. No seasonal traffic adjustment factor was applied to the test data.

Four methods discussed below were used to predict the average values of ADT, ADTT, EALs and truck EALs over the anticipated life of the bridge (through year 2038). Those methods are used to estimate the bridge loading in terms of average stress range and frequency of stress cycles. For each test location, the remaining safe life was calculated by different methods using combinations of RMS and RMC stresses, total traffic and truck traffic, providing four safe-life estimates at each test location as shown in Tables 4 through 7.

Method A - It was estimated that a traffic volume (ADT) of 70,000 vehicles was the maximum capacity of a six-lane rural interstate highway for a Class C level of service (according to the Highway Capacity Manual). Based upon the traffic growth equation, it was estimated that by the year 2019 the ADT would reach the 70,000-vehicle limit. Therefore, it was assumed that the ADT would remain constant at 70,000 vehicles through the year 2038. Average ADT, ADTT, EALs, and truck EALs were calculated based upon the those assumptions. The number of stress cycles per year were assumed to be proportional to the number of stress cycles recorded during the one-week test periods. The number of stress cycles per year was multiplied by an ADT

adjustment factor to calculate the average number of stress cycles per year over the anticipated life of the bridge (1966 to 2038). The constant-amplitude stress ranges calculated by RMS and RMC methods were multiplied by EAL adjustment factors to get modified constant-amplitude stress ranges. Those were used to calculate the total life cycles by an equation derived for the AASHTO category E fatigue details for nonredundant members. Remaining life was calculated by dividing the total life cycles by the number of stress cycles per year and by deducting the past life (22 years).

Method B - The bridge loading magnitudes and frequencies were considered to increase as previously discussed for Method A. The EAL and ADT values were averaged over two time periods, 1966 to 1988 and 1988 to 2038. The first time period represents prior damage (or service life expended) and the second time period represents the predicted future damage. EAL and ADT adjustment factors were calculated for both time periods by dividing the average EALs and ADT during those periods by the projected 1988 EALs and ADT, respectively. Those adjustment factors were used to calculate the modified constant-amplitude stresses and the number of stress cycles per year respectively, for those time periods. An equivalent constant-amplitude stress was derived for the anticipated life of the bridge (1966 to 2038) by taking the weighted average of the constant-amplitude stresses for two time periods based upon the number of stress cycles in those time periods. That stress was used to calculate total life cycles (as in method A). The remaining life was determined by subtracting the number of stress cycles during the prior life of the bridge (1966 to 1988) from the total life cycles and then dividing it by the projected number of stress cycles for the future (1988 to 2038).

Method C - Linear regression was used to determine the increase in ADT and EALs from 1966 to 2038. That method predicted a total ADT of 88,800 and an EAL of 22,670 in the year 2038. The predicted ADTT in the year 2038 was 20,200 with Truck EAL of 22,430. Actually, this would require an increase of two lanes over the proposed six-lane structure. Average EAL and ADT values between 1966 and 2038 were determined and adjusted by dividing them by the projected 1988 values. Calculation of remaining lives at each test location followed Method A.

Method D - The effects of changes in ADT and EALs over the life of the bridge were neglected and the present values of constant-amplitude RMS and RMC stresses were used for calculating the remaining life of the bridge. Calculation of remaining lives at each test location followed method A.

In most cases, adjusted equivalent stress ranges (RMS and RMC) for each test location were less than the 2.5-ksi endurance limit used by AASHTO for category E details on nonredundant members. However, some stress cycles at each location exceeded the 2.5-ksi endurance limit. That indicated finite service lives were possible even though the equivalent stresses were below the endurance limit. That was accommodated by extending the sloped (finite life) portion of the S-N curve below the endurance limit (3). That yields finite service lives for such cases (though service lives may be quite long for cases such as the I 75 bridge where percentages of the load cycles above the endurance limit are very low at each test location).

Table 4 provides the least conservative (most optimistic) predictions for safe-life performance. As previously noted, RMS equivalent stress ranges closely approximate fatigue behavior of variable-amplitude stress spectrum. The total ADT and EAL adjustment factors are low. For load-prediction methods A, B and D, all the test locations provide safe lives well over 50 years. Only test location 2 shows less than 50 years (42 years) of service-life for load-prediction method C.

The remaining safe lives predicted by Table 5 are based upon RMS equivalent stress ranges and truck traffic. As with the predictions derived in Table 4, all of those in Table 5 provide safe lives in excess of 50 years except at test location 2 using load-prediction method C.

Table 6 provides a more conservative fatigue life based upon total traffic and the RMC equivalent stress. All load-prediction methods provide safe lives greater than 50 years, except at test locations 1, 2, 5 and 6 by load-prediction method C. For those cases, the safe-life predictions range from 18 to 44 years.

Table 7 is also more conservative, and is based upon truck traffic and the RMC equivalent stress. The safe-life values are all equal to or slightly less than those predicted for total traffic in Table 6 except for prediction method C. The safe-life predictions exceed 50 years, except at test locations 1, 2, 5 and 6 by load-prediction method C. For those cases, the safe-life predictions range from 15 to 47 years.

FATIGUE-CRACK GROWTH ANALYSES

WSA personnel informed KTC personnel that close visual inspections of the connections revealed some cracks in the gusset plate to girder fillet welds. However, those cracks were said to be in the weld to gusset plate areas and did not penetrate into the base metal of the girders. KTC personnel were not informed of any further details of the cracking problem.

Due to presence of cracks in the structure, KTC personnel performed fatigue-crack growth analyses with several preliminary assumptions to estimate a level of inspection that would insure structural integrity at the welded connections. A fatigue-crack growth software program, LICAFF, developed by FractuREsearch Corporation of Galena, Ohio was used to predict crack growth. The empirically deduced Paris model used in LICAFF was most suitable for modeling the fatigue-crack growth for a known constant-amplitude cyclic stress applied across the crack tips. It neglects the retardation effect at the tip of a growing crack, thus providing conservative estimate of the crack growth rate.

Paris model is given by equation:

$$da/dN = Cp\ (\Delta K)^{Mp} \qquad (5)$$

where

da/dN = increment of crack growth (inches per cycle)

ΔK = change in stress intensity due to cyclic stress (ksi in)

and Cp, Mp = material constants.

The LICAFF program was run with the following parameters:

Crack Geometry	= Single-edge crack
Tension Yield Stress	= 33 ksi
Plate Thickness	= 0.5 inches
Plate Width	= Infinite
Initial Crack Size	= 1.0 inches
Final Crack Size	= 6.0 inches
Constant-Amplitude Stress Range	= 0 ksi minimum stress (ksi); Sre_{rmc} maximum stress (ksi)
Cp	= 3.6×10^{-10}
Mp	= 3.

The initial crack was assumed to be a through crack growing as a single-edge crack through the steel. The material was ASTM A 373 steel with a yield strength of 33 ksi. The material thickness was assumed to be 1/2 inch. Various plate thicknesses occur in the webs of the upper and lower chord members, but they do not effect the crack-growth model. The plate width was assumed to be infinite to simplify the analysis. However, that simplification may be slightly less conservative than using the actual dimensions of the truss members. The equation constants Cp and Mp are given to be 3.6×10^{-10} and 3 respectively (in English units) for pearlitic-ferritic steels such as ASTM A 373 (4). Those values are considered conservative by others (5,6). The minimum stress was 0 ksi. The constant amplitude RMC stress value for each location was used as the maximum stress. Those values are given in Table 2. No stress adjustment factor of the type employed in the safe-life analyses were used.

A one-inch crack was hypothesized as the initial crack size based on the assumption that the recent inspection would reliably detect larger cracks. Fisher has stated that visual inspection can be reliably detect smaller surface-breaking flaws (7). However, since the bridge inspectors used on I 75 bridge were not prequalified to reliably detect cracks down to a given minimum size, the one-inch minimum crack detection limit is not unreasonable. No fracture-mechanics calculations were used to estimate the critical crack length for structural failure. A six-inch long crack was hypothesized for the final crack size (i.e., the crack size for the structural failure). That assumption would probably entail brittle or quasi-brittle cracking. Failure of a structural member by ductile fracture (net section yielding) would require a crack at least twice as long.

Program runs were conducted using equation 5 for test locations 1 through 6 using Sre_{rmc} stress ranges from Table 2. Tables 8-15 contain tabulations of crack growth and number of stress cycles for each test location. The number of years required to propagate the crack from 1 to 6 inches was determined by dividing the total number of stress cycles by the equivalent number of stress cycles per year determined for each test location based on present loading frequency. Those results are listed in Table 16. The derived data indicates long time intervals to grow the hypothetical cracks to 6 inches. The shortest anticipated interval (test location 2-first test) is 364 years. Typically, the fatigue cracks have a slow initial fatigue-crack growth rate. The Paris equation predicts that 70 percent of the total stress cycles will be required

for the first two inches of crack growth (from 1 to 3 inches). For test location 2 (first test) the equation predicts that initial crack growth would require approximately 255 years.

However, there is reason to believe that fatigue-crack growth rate may exceed that predicted by the Paris equation using the constants for pearlitic-ferritic steels (8). The presence of moisture and/or chlorides at crack tip can exacerbate the fatigue-crack growth. The crack growth rate can increase as much as 10 times over the rate determined in a laboratory environment (9). That is especially true in long-term corrosion situations where corrodants can be effective. For test location 2 that increase in the corrosion rate could possibly decrease the time to grow the hypothetical crack to 36.4 years. It should be noted that corrosion effects would not affect the safe-life analyses as usually no surface cracks are present on a bridge until approximately 90 percent of the safe life is expended.

CONCLUSIONS

The safe-life analyses provided by prediction method B in Tables 4 through 7 indicate that the southbound I 75 bridge over the Kentucky River should not be prone to fatigue failure within the next 50-60 years at the six test locations. The less conservative load-prediction methods (A and D) provide safe lives in excess of 300 years for all test locations even by using the more conservative root-mean cube equivalent-stress summing equation. The most conservative load-prediction method C provides the lowest safe-life estimates (down to 15 years).

Since load-prediction method C is not a practical scenario (it anticipates excessive traffic over the bridge) it is probably too conservative to be considered as realistic. If this assumption is accepted, then it is likely that the structure could used in the new six-lane bridge (if the six test locations are the "worst-case" examples of those connections).

It should be restated that the strain-gage readings are believed to be conservative. That is based upon comparisons between the shunt-calibrated stress values derived in the field and the laboratory-derived values. Therefore, it is unlikely that any analytical errors were incurred due to low strain-gage readings.

It was observed that predictions of future loads have significant impact on the safe-life analyses. The only means of confirming the accuracy of the

KYDOH and KTC loading and ADT estimates will be to re-test the structure in the future. If heavier loads are encountered than presently envisioned, the fatigue situation will need to be re-evaluated and closer inspection techniques may be necessary. However, that would not mean that the structure would have to be scrapped in the future.

The safe-life analyses would be obviated by the presence of growing fatigue cracks in the base metal of the major structural members. If that were the case, a comprehensive fatigue-crack growth/fracture mechanics/NDT analyses would be necessary.

The cracks detected at the gusset-plate connections did not penetrate into the base metal of the major structural members. Therefore, the presence of cracks does not invalidate the safe-life analyses.

The fatigue-crack growth analyses predict slow growth rates for small 1-inch long cracks in the present loading environment. The analyses is not as complete as KTC personnel would desire. However, it is sufficient to indicate that a small cracks would grow slowly at any of the test sites unless very unusual conditions existed on the bridge.

KTC personnel are not certain of the size of any cracks that might remain undetected in the bridge. Also, KTC personnel are not certain of the maximum crack size that could be tolerated in the nonredundant structural members of the bridge. If the truss is to be used in the future those should be ascertained.

Two options can be considered for minimizing or eliminating the possibility of fatigue failure if the truss is to be retained on the bridge in future. First, the gusset welds can be removed and gussets can be bolted to the structural members. That would increase the fatigue resistance of the connections to AASHTO category B which should preclude the initiation of fatigue cracks. Locations where the welds were removed should be ground flush and subjected to close NDT-enhanced inspection to insure no cracks are present in the base metal of the chord members or bracing.

Below a threshold fatigue stress intensity, no fatigue cracking will occur (10). That is given by the equation:

$$Kre = C\ Sre\sqrt{\pi a} \qquad (6)$$

where:

Kre = fatigue stress intensity at a crack tip (ksi in.)

C = constant for crack geometry and disposition in a structural detail

Sre = equivalent single-amplitude stress range (ksi)

a = crack length in inches.

A NDT method can be employed that will reliably detect cracks down to a very small crack length (a) in the base metal. If none are detected, then, due to the low values of a and Sre, Kre at the connections will be below the threshold stress intensity necessary to initiate for fatigue-crack growth. Any small cracks detected by nondestructive testing can be eliminated by grinding or coring. Further analytical work would be necessary to determine a suitable NDT method and prequalify the NDT personnel to ensure reliable crack detection.

The second option would be to leave the gusset welds intact and periodically subject the welds to close inspection accompanied with a comprehensive fatigue-crack growth/fracture mechanics/NDT analyses. That analyses would include determination of the minimum crack size that a chosen NDT method could reliably detect as well the maximum crack size the bridge could tolerate without failure.

Once the revised six-lane bridge is reopened (with the gusset-plate welds intact), it would be strain-gaged again and also subjected to non-destructive inspection (visual or NDT-enhanced). That should be done no later than 5 years after the revised structure is opened to traffic. After the base-line nondestructive inspection and analyses, it is likely that the welded connections would not need to be re-inspected closely more than once every 10 years (and possibly at longer intervals). The nondestructive inspection and analyses might eliminate some connections from requiring further close inspections.

The analyses and inspections proposed for the particular truss connections in the two preceding options are in accordance with section 2.3 of the AASHTO "Manual for Maintenance Inspection of Bridges -1983" as contained in the 1986 AASHTO "Revisions to the Manual for Maintenance Inspection of Bridges". That section requires a state to develop an inspection plan that contains the rationale for inspection and to outline the details of the level of inspections to be performed. The inspections previously proposed are specific only for the welded gusset-plate connections. They are recommended to supplement rather than supplant the FHWA-mandated biennial inspections.

It is possible that the cracks previously detected in the gusset welds are benign. However, it would be desirable to retrofit those cracks by placing check-holes at the crack tips and possibly by augmenting the check-holes with splice plates lapped across the cracks. Those repairs may appear to be unessential, but the consequences of failure of the nonredundant structural members due to cracking are unacceptable. Too many pertinent factors related to the possible fracture of those bridge members are unknown. They must be compensated for by conservative repair policies.

If the six test locations strain-gaged and analyzed are representative (or worst-case) examples of the remaining gusset connections, the bridge should be in a reasonably good condition from fatigue standpoint at the gusset connections to allow its continued use if that proves financially beneficial to KYDOH. However, follow-up analyses and inspections will be necessary to insure its immunity from fatigue problems in future.

REFERENCES

1. Hopwood, T. II, Oka, V. G., Deen, R. C., "Reliability Assessment of High-Risk Steel Bridges by Nondestructive Test Methods", University of kentucky Transportation Research Program, Research Report UKTRP-87-27, October 1987.

2. Ecton, D. L., Memorandum from Kentucky Transportation Cabinet, Division of Planning, Dated April 27, 1987.

3. Fisher, J. W., Mertz, D. R., Zhong, A., "Steel Bridge Members Under Variable Amplitude Long Life Fatigue Loading", National Cooperative Research Program, Report No. 267, Transportation Research Board, Washington, DC, December 1983.

4. Rolfe, S. T., and Barsom, J. M., "Fracture and Fatigue Control in Structures", Prentice-Hall Inc., Englewood Cliffs, NJ, 1977, PP. 239.

5. Moses, F., Schulling, C. G., and Raju, K. S., "Fatigue Evaluation Procedures for Steel Bridges", National Cooperative Highway Research Program, Report No. 267, Transportation Research Board, Washington, DC, December 1983.

6. Fisher, J. W., "Fatigue and Fracture in Steel Bridges", John Wiley and Sons, New York, NY, 1984, PP. 8.

7. Fisher, J. W., Hausammann, H., Sullivan, M. P., and Pense, A. W., "Detection and Repair of Fatigue Damage in Welded Highway Bridges", Lehigh University, National Cooperative Highway Research Program, Report No. 206, Transportation Research Board, Washington, DC, June 1979, PP. 48.

8. Fuchs, H. O., and Stephans, R. I., "Metal Fatigue in Engineering", John Wiley and Sons, New York, NY, 1980, PP 87.

9. Op. Cit. 8, PP 220.

10. Op. Cit. 5, PP 61.

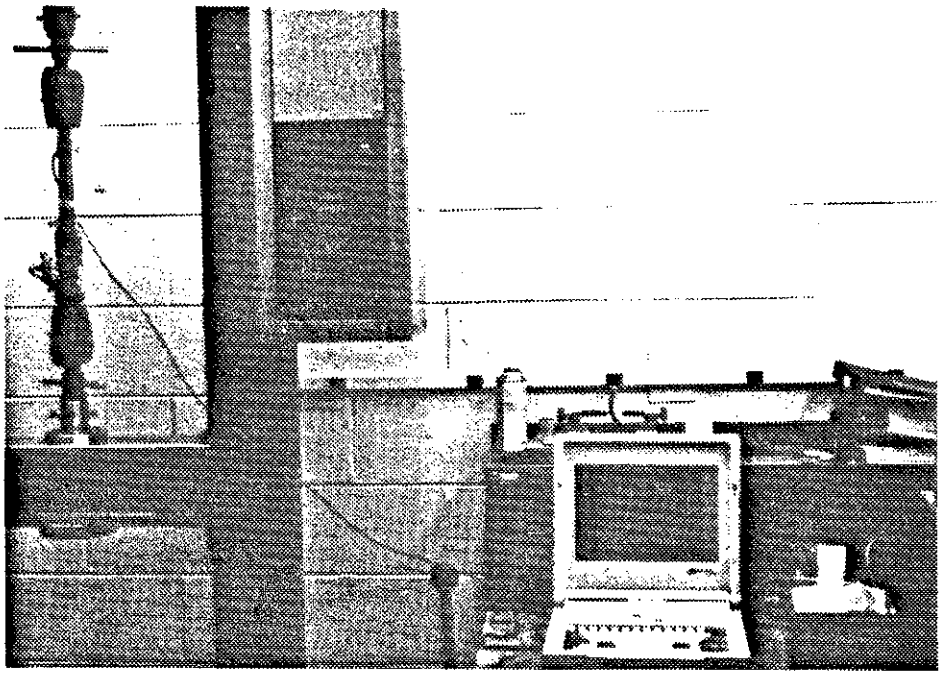

Figure 1 : Strain-Gage Calibration

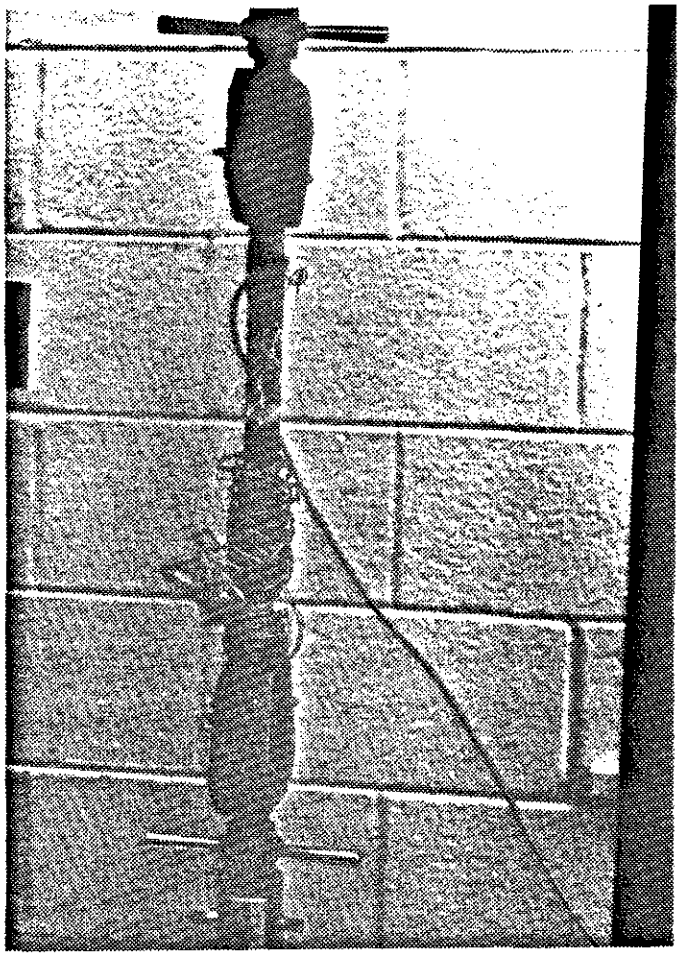

Figure 2: Test Bar with Strain Gages

TABLE 1 : STRESS-RANGE DATA FROM STRAIN-GAGE TESTS

A. TEST LOCATION 1 : U3L4
TEST BEGINS : 7/27/1988 AT 11:23:04
TEST DURATION : 590,735 SECONDS
SAMPLE RATE : 50

STRESS-RANGE IN KSI	NUMBER OF CYCLES
0-1	9,049
1-2	3,335
2-3	23
3-4	13
4-5	1
5-6	1

B. TEST LOCATION 2 : LOWER CHORD - L4L6
TEST BEGINS : 7/13/1988 AT 11:22:38
TEST DURATION : 231,524 SECONDS
SAMPLE RATE : 50

STRESS-RANGE IN KSI	NUMBER OF CYCLES
0-1	4,006
1-2	1,824
2-3	63
3-4	2
4-5	3
7-8	1

C. TEST LOCATION 3 : UPPER CHORD - U5U7
TEST BEGINS : 7/13/1988 AT 11:31:14
TIME DURATION : 597,472 SECONDS
SAMPLE RATE : 50

STRESS-RANGE IN KSI	NUMBER OF CYCLES
0-1	8,136
1-2	688
2-3	17
3-4	12
4-5	4
5-6	3

TABLE 1 : STRESS-RANGE DATA FROM STRAIN-GAGE TESTS

D. TEST LOCATION 4 : U13U15
TEST BEGINS : 7/27/1988 AT 11:10:08
TEST DURATION : 592,663 SECONDS
SAMPLE RATE : 50

STRESS-RANGE IN KSI	NUMBER OF CYCLES
0-1	1,610
1-2	27
2-3	3
3-4	37
4-5	3
5-6	4

E. TEST LOCATION 5 : BOTTOM CHORD L14L16
TEST BEGINS : 7/20/1988 AT 10:03:15
DURATION : 607,474 SECONDS
SAMPLE RATE : 50

STRESS-RANGE IN KSI	NUMBER OF CYCLES
0 -1.2	10,947
1.2-2.4	1,882
2.4-3.6	52
3.6-4.8	5
4.8-6.0	1
8.4-9.6	1

F. TEST LOCATION 6 : DIAGONAL L16U17
TEST BEGINS : 7/20/1988 AT 10:15:26
TEST DURATION : 605,664 SECONDS
SAMPLE RATE : 50

STRESS-RANGE IN KSI	NUMBER OF CYCLES
0-1	13,768
1-2	3,718
2-3	30
3-4	3
4-5	3
6-7	3

TABLE 1 : STRESS-RANGE DATA FROM STRAIN-GAGE TESTS

G. TEST LOCATION 2 : LOWER CHORD L4L6 (NEW TEST)
TEST BEGINS : 8/3/1988 AT 9:49:10
TEST DURATION : 602,407 SECONDS
SAMPLE RATE : 50

STRESS RANGE IN KSI	NUMBER OF CYCLES
0 -1.2	10,351
1.2-2.4	2,376
2.4-3.6	48
3.6-4.8	1
4.8-6.0	6
6.0-7.2	5
7.2-8.4	1

H. TEST LOCATION 4 : U13U15 (NEW TEST)
TEST BEGINS : 8/10/1988 AT 15:39:16
TEST DURATION : 954,006 SECONDS
SAMPLE RATE : 50

STRESS-RANGE IN KSI	NUMBER OF CYCLES
0-1	1,198
1-2	48
2-3	6
3-4	96
4-5	1

TABLE 2 : ROOT MEAN SQUARE (RMS) AND ROOT MEAN CUBE (RMC) STRESSES AT DIFFERENT TEST LOCATIONS.

TEST LOCATION	RMS STRESS (KSI)	RMC STRESS (KSI)	TOTAL NUMBER OF CYCLES	TEST DURATION (SECONDS)
1	0.9026	1.0300	12,422	590,735
2	0.9780	1.1260	5,899	231,524
3	0.6730	0.8250	8,860	597,472
4	0.8144	1.1940	1,684	592,663
5	0.9110	1.0750	12,888	607,474
6	0.8350	0.9700	17,525	606,143
2(NEW TEST)	0.9820	1.1670	12,788	602,407
4(NEW TEST)	1.1030	1.5070	1,349	954,006

TABLE 3 : ADT AND EAL ADJUSTMENT FACTORS

	TOTAL ADT	TRUCK ADT ONLY
METHOD A		
ADT FACTOR	0.9498	0.9680
EAL FACTOR	1.0680	1.0120
METHOD B		
ADT FACTOR PAST*	0.6613	0.6540
ADT FACTOR FUTURE**	1.3740	1.3950
EAL FACTOR PAST	0.5811	0.5783
EAL FACTOR FUTURE	1.6000	1.5360
METHOD C		
ADT FACTOR	1.3530	1.4890
EAL FACTOR	1.7190	1.7110
METHOD D		
ADT FACTOR	1.0000	1.0000
EAL FACTOR	1.0000	1.0000

* 1966 to 1988
** 1988 to 2038

TABLE 4 : REMAINING FATIGUE LIFE IN YEARS BASED ON RMS STRESS AND TOTAL ADT

TEST LOCATION	METHOD	A	B	C	D
1		668	176	80	791
2		416	108	42	494
3		2,535	682	356	2,990
4		7,133	1,929	1,021	8,405
5		642	169	76	760
6		626	165	73	741
2(NEW TEST)		497	130	54	589
4(NEW TEST)		5,311	1,435	767	6,258

TABLE 5 : REMAINING FATIGUE LIFE IN YEARS BASED ON RMS STRESS AND TRUCK ADT

TEST LOCATION	METHOD	A	B	C	D
1		786	196	72	791
2		491	121	37	494
3		2,970	757	327	2,990
4		8,350	2,136	955	8,405
5		755	188	68	760
6		736	184	66	741
2(NEW TEST)		585	145	48	589
4(NEW TEST)		6,218	1,589	706	6,258

TABLE 6 : REMAINING FATIGUE LIFE IN YEARS BASED ON RMC STRESS AND TOTAL ADT

TEST LOCATION	METHOD	A	B	C	D
1		426	111	44	506
2		254	64	18	303
3		1,292	345	172	1,525
4		2,025	544	281	2,390
5		364	94	35	433
6		375	97	36	445
2(NEW TEST)		273	69	21	325
4(NEW TEST)		1,900	510	262	2,241

TABLE 7 : REMAINING FATIGUE LIFE IN YEARS BASED ON RMC STRESS AND TRUCK ADT

TEST LOCATION	METHOD	A	B	C	D
1		502	124	39	506
2		301	72	15	303
3		1,515	383	157	1,525
4		2,384	604	257	2,390
5		430	105	30	433
6		442	108	32	445
2(NEW TEST)		323	78	18	325
4(NEW TEST)		2,227	566	240	2,241

Table 8 : Crack Growth at Test Location 1 by Fatigue-Crack Growth Software Program LICAFF

Constant-Amplitude Maximum Stress = 1.030 Ksi
Minimum Stress = 0.000 Ksi

Number of Load Cycles per Year at Test Location 1 based on the Test Duration and Number of Cycles in the Test Duration = 663,140

Crack Length Inches	Load Cycles by LICAFF	Years Based on Number of Load Cycles per Year
1.0000	0	0.00
1.1268	37,407,310	56.40
1.2697	72,649,320	109.55
1.4308	105,851,700	159.62
1.6122	137,132,600	206.79
1.8167	166,603,700	251.23
2.0471	194,369,900	293.10
2.3067	220,530,100	332.55
2.5993	245,177,600	369.72
2.9289	268,400,000	404.74
3.3004	290,280,000	437.73
3.7190	310,895,400	468.82
4.1906	330,319,700	498.11
4.7221	348,621,700	525.71
5.3210	365,866,500	551.71
5.9958	382,115,200	576.22
6.0000	382,115,200	576.22

Table 9 : Crack Growth at **Test Location 2** by Fatigue-Crack Growth Software Program LICAFF

Constant-Amplitude Maximum Stress = 1.126 Ksi
Minimum Stress = 0.000 Ksi

Number of Load Cycles per Year at **Test Location 2** based on the Test Duration and Number of Cycles in the Test Duration = 803,506

Crack Length Inches	Load Cycles by LICAFF	Years Based on Number of Load Cycles per Year
1.0000	0	0.00
1.1268	28,632,080	35.63
1.2697	55,606,810	69.20
1.4308	81,020,330	100.83
1.6122	104,963,200	130.63
1.8167	127,520,800	158.70
2.0471	148,773,400	185.15
2.3067	168,796,900	210.07
2.5993	187,662,300	233.55
2.9289	205,437,100	255.67
3.3004	222,184,400	276.51
3.7190	237,963,800	296.15
4.1906	252,831,400	314.66
4.722	266,840,000	322.09
5.3210	280,039,400	348.52
5.9958	292,476,300	364.00
6.0000	292,476,300	364.00

Table 10 : Crack Growth at **Test Location 3** by Fatigue-Crack Growth Software Program LICAFF

Constant-Amplitude Maximum Stress = 0.825 Ksi
Minimum Stress = 0.000 Ksi

Number of Load Cycles per Year at **Test Location 3** based on the Test Duration and Number of Cycles in the Test Duration = 467,652

Crack Length Inches	Load Cycles by LICAFF	Years Based on Number of Load Cycles per Year
1.0000	0	0.00
1.1268	72,795,780	155.66
1.2697	141,377,800	302.31
1.4308	205,990,600	440.47
1.6122	266,864,300	570.64
1.8167	324,216,000	693.28
2.0471	378,249,900	808.82
2.3067	429,158,500	917.68
2.5993	477,123,200	1020.25
2.9289	522,314,700	1116.88
3.3004	564,893,800	1207.93
3.7190	605,012,200	1293.72
4.1906	642,812,500	1374.55
4.7221	678,428,800	1450.71
5.3210	711,987,600	1522.47
5.9958	743,608,000	1590.08
6.0000	743,608,000	1590.08

Table 11 : Crack Growth at **Test Location 4** by Fatigue-Crack Growth Software Program LICAFF

Constant-Amplitude Maximum Stress = 1.194 Ksi
Minimum Stress = 0.000 Ksi

Number of Load Cycles per Year at **Test Location 4** based on the Test Duration and Number of Cycles in the Test Duration = 89,607

Crack Length Inches	Load Cycles by LICAFF	Years Based on Number of Load Cycles per Year
1.0000	0	0.00
1.1268	24,013,480	267.98
1.2697	46,636,960	520.46
1.4308	67,951,060	758.32
1.6122	88,031,760	982.42
1.8167	106,950,600	1193.55
2.0471	124,775,000	1392.46
2.3067	141,568,500	1579.88
2.5993	157,390,800	1756.45
2.9289	172,298,400	1922.82
3.3004	186,344,200	2079.57
3.7190	199,578,200	2227.26
4.1906	212,047,500	2366.41
4.7221	223,796,500	2497.53
5.3210	234,866,700	2621.07
5.9958	245,297,500	2737.48
6.0000	245,297,500	2737.48

Table 12 : Crack Growth at **Test Location 5** by Fatigue-Crack Growth Software Program LICAFF

Constant-Amplitude Maximum Stress = 1.075 Ksi
Minimum Stress = 0.000 Ksi

Number of Load Cycles per Year at **Test Location 5** based on the Test Duration and Number of Cycles in the Test Duration = 669,059

Crack Length Inches	Load Cycles by LICAFF	Years Based on Number of Load Cycles per Year
1.0000	0	0.00
1.1268	32,903,540	49.17
1.2697	63,902,480	95.51
1.4308	93,107,290	139.16
1.6122	120,622,100	180.28
1.8167	146,544,900	219.03
2.0471	170,968,100	255.53
2.3067	193,978,700	289.92
2.5993	215,658,600	322.33
2.9289	236,085,000	352.86
3.3004	255,330,700	381.62
3.7190	273,464,200	408.72
4.1906	290,549,700	434.26
4.7221	306,648,200	458.32
5.3210	321,816,800	481.00
5.9958	336,109,100	502.36
6.0000	336,109,100	502.36

Table 13 : Crack Growth at **Test Location 6** by Fatigue-Crack Growth Software Program LICAFF

Constant-Amplitude Maximum Stress = 0.970 Ksi
Minimum Stress = 0.000 Ksi

Number of Load Cycles per Year at **Test Location 6** based on the Test Duration and Number of Cycles in the Test Duration = 911,779

Crack Length Inches	Load Cycles by LICAFF	Years Based on Number of Load Cycles per Year
1.0000	0	0.00
1.1268	44,787,090	49.12
1.2697	86,981,710	95.39
1.4308	126,734,300	139.00
1.6122	164,186,400	180.07
1.8167	199,471,600	218.77
2.0471	232,715,600	255.23
2.3067	264,036,700	289.58
2.5993	293,546,700	321.94
2.9289	321,350,400	352.44
3.3004	347,547,000	381.17
3.7190	372,229,500	408.24
4.1906	395,485,900	433.75
4.7221	417,398,600	457.78
5.3210	438,045,500	480.42
5.9958	457,499,700	501.76
6.0000	457,499,700	501.76

Table 14 : Crack Growth at Test Location 2 (NEW TEST) by Fatigue-Crack Growth Software Program LICAFF

Constant-Amplitude Maximum Stress = 1.167 Ksi
Minimum Stress = 0.000 Ksi

Number of Load Cycles per Year at Test Location 2 (NEW TEST) based on the Test Duration and Number of Cycles in the Test Duration = 669,452

Crack Length Inches	Load Cycles by LICAFF	Years Based on Number of Load Cycles per Year
1.0000	0	0.00
1.1268	25,719,090	38.41
1.2697	49,949,430	74.61
1.4308	72,777,400	108.71
1.6122	94,284,370	140.83
1.8167	114,547,000	171.10
2.0471	133,637,400	199.62
2.3067	151,623,600	226.48
2.5993	168,569,800	251.80
2.9289	184,536,100	275.65
3.3004	199,579,500	298.12
3.7190	213,753,500	319.29
4.1906	227,108,600	339.24
4.7221	239,692,000	358.04
5.3210	251,548,500	375.75
5.9958	262,720,100	392.44
6.0000	262,720,100	392.44

Table 15 : Crack Growth at **Test Location 4 (NEW TEST)** by
Fatigue-Crack Growth Software Program LICAFF

Constant-Amplitude Maximum Stress = 1.507 Ksi
Minimum Stress = 0.000 Ksi

Number of Load Cycles per Year at **Test Location 4 (NEW TEST)**
based on the Test Duration and Number of Cycles in the
Test Duration = 44,593

Crack Length Inches	Load Cycles by LICAFF	Years Based on Number of Load Cycles per Year
1.0000	0	0.00
1.1268	11,943,410	267.83
1.2697	23,195,480	520.15
1.4308	33,796,320	757.88
1.6122	43,783,720	981.85
1.8167	53,193,260	1192.86
2.0471	62,058,450	1391.66
2.3067	70,410,890	1578.96
2.5993	78,280,350	1755.44
2.9289	85,694,780	1921.70
3.3004	92,680,630	2078.36
3.7190	99,262,750	2225.97
4.1906	105,464,500	2365.04
4.7221	111,308,000	2496.08
5.3210	116,813,900	2619.55
5.9958	122,001,800	2735.89
6.0000	122,001,800	2735.89

Table 16 : Fatigue-Crack Growth Estimation

Test Location	Test Duration Seconds	Number of Load Cycles in Test Duration	Number of Load Cycles per Year	NCTF by LICAFF	Life in Years
1	590,735	12,422	663,140	382,115,200	576.22
2	231,524	5,899	803,506	292,476,300	364.00
3	597,472	8,860	467,652	743,608,000	1590.08
4	592,663	1,684	89,607	245,297,500	2737.48
5	607,474	12,888	669,059	336,109,100	502.36
6	606,143	17,525	911,779	457,499,700	501.77
2(New Test)	602,407	12,788	669,452	262,720,100	392.44
4(new Test)	954,006	1,349	44,593	122,001,800	2735.90

NCTF : Number of load cycles for a hypothetical crack of 1-inch intial size to grow to a critical size of 6 inches, calculated by LICAFF fatigue-crack growth software.

APPENDIX

American Association of State Highway
and Transportation Officials (AASHTO)
Fatigue Design Tables

Reference : AASHTO Standard Specifications
for Highway Bridges, Thirteenth Edition,1983
Section 10.3 , Page 109

TABLE 10.3.1A Allowable Fatigue Stress Range

Redundant Load Path Structures*

Category See Table 10.3.1B	Allowable Range of Stress, F_{sr} (ksi)[a] For 100,000 Cycles	For 500,000 Cycles	For 2,000,000 Cycles	For over 2,000,000 Cycles
A	60	36	24	24
B	45	27.5	18	16
C	32	19	13	10
				12[b]
D	27	16	10	7
E	21	12.5	8	5
E′	16	9.4	5.8	2.6
F	15	12	9	8

Nonredundant Load Path Structures

Category See Table 10.3.1B	Allowable Range of Stress, F_{sr} (ksi)[a] For 100,000 Cycles	For 500,000 Cycles	For 2,000,000 Cycles	For over 2,000,000 Cycles
A	36	24	24	24
B	27.5	18	16	16
C	19	13	10	9
			12[b]	11[b]
D	16	10	7	5
E[c]	12.5	8	5	2.5
F	12	9	8	7

*Structure types with multi-load paths where a single fracture in a member cannot lead to the collapse. For example, a simply supported single span multi-beam bridge or a multi-element eye bar truss member has redundant load paths.

[a]The range of stress is defined as the algebraic difference between the maximum stress and the minimum stress. Tension stress is considered to have the opposite algebraic sign from compression stress.

[b]For transverse stiffener welds on girder webs or flanges.

[c]Partial length welded cover plates shall not be used on flanges more than 0.8 inches thick for nonredundant load path structures.